Antiangiogenesis Enhances Intratumoral Drug Retention

Jie Ma, Chong-Sheng Chen, Todd Blute, and David J. Waxman

Abstract

The tumor vasculature delivers nutrients, oxygen, and therapeutic agents to tumor cells. Unfortunately, the delivery of anticancer drugs through tumor blood vessels is often inefficient and can constitute an important barrier for cancer treatment. This barrier can sometimes be circumvented by antiangiogenesis-induced normalization of tumor vasculature. However, such normalizing effects are transient; moreover, they are not always achieved, as shown here, when 9L gliosarcoma xenografts were treated over a range of doses with the VEGF receptor-selective tyrosine kinase inhibitors axitinib and AG-028262. The suppression of tumor blood perfusion by antiangiogenesis agents can be turned to therapeutic advantage, however, through their effects on tumor drug retention. In 9L tumors expressing the cyclophosphamide-activating enzyme P450 2B11, neoadjuvant axitinib treatment combined with intratumoral cyclophosphamide administration significantly increased tumor retention of cyclophosphamide and its active metabolite, 4-hydroxycyclophosphamide. Similar increases were achieved using other angiogenesis inhibitors, indicating that increased drug retention is a general response to antiangiogenesis. This approach can be extended to include systemic delivery of an anticancer prodrug that is activated intratumorally, where antiangiogenesis-enhanced retention of the therapeutic metabolite counterbalances the decrease in drug uptake from systemic circulation, as exemplified for cyclophosphamide. Importantly, the increase in intratumoral drug retention induced by neoadjuvant antiangiogenic drug treatment is shown to increase tumor cell killing and substantially enhance therapeutic activity *in vivo*. Thus, antiangiogenic agents can be used to increase tumor drug exposure and improve therapeutic activity following intratumoral drug administration, or following systemic drug administration in the case of a therapeutic agent that is activated intratumorally. *Cancer Res; 71(7); 2675–85. ©2011 AACR.*

Introduction

The tumor vasculature is often characterized by low vascularity, poor organization, and abnormal morphology, which results in inefficient transport of oxygen and therapeutic agents into tumors and constitutes a substantial barrier to effective cancer treatment (1). Extensive efforts have been made to improve tumor drug uptake by developing new delivery vehicles or increasing tumor vascular patency (2, 3). The growth and expansion of many tumors is associated with pathological angiogenesis stimulated by VEGF, which is a validated therapeutic target for cancer treatment. Bevacizumab, a neutralizing antibody for human VEGF, is an antiangiogenic drug that increases the survival of patients with metastatic colorectal cancer and non-small-cell lung cancer when given in combination with conventional chemotherapy (4, 5). Small-molecule receptor tyrosine kinase inhibitors (RTKIs) that inhibit VEGF

receptors (VEGFR) can also be used to induce antiangiogenesis. However, despite efficacy observed in clinical trials with several such RTKIs (6, 7), recent phase III trials showed very limited benefits when antiangiogenic RTKIs were combined with conventional chemotherapy (8–10). These observations raise the question as to how antiangiogenesis treatments affect tumor uptake of other chemotherapeutic agents and the overall antitumor activity of combination therapies.

Morphological normalization of surviving tumor blood vessels has been observed following treatment with a variety of antiangiogenic drugs (11). It has been proposed that antiangiogenesis may transiently normalize the tumor vasculature, leading to an increase in tumor drug uptake (12). Like the antiangiogenic antibodies bevacizumab and DC101, the VEGF receptor-selective RTKI axitinib (13) induces morphological normalization of the tumor vasculature and can increase the transport efficiency of individual blood vessels that survive antiangiogenesis treatment (14, 15). However, the total number of surviving blood vessels decrease and overall tumor blood perfusion is not improved by axitinib treatment, as indicated by the increase in tumor hypoxia and the decrease in tumor uptake of small molecules, including 4-OH-CPA, the active metabolite of the anticancer prodrug cyclophosphamide (CPA; refs. 14, 16). This lack of improved tumor vascular functionality ("normalization") by axitinib and certain other antiangiogenic drugs (17–20) could be the result of doses that are optimized for maximal angiogenesis inhibition with acceptable host toxicity

Authors' Affiliation: Division of Cell and Molecular Biology, Department of Biology, Boston University, Boston, Massachusetts

Note: Supplementary data for this article are available at Cancer Research Online (http://cancerres.aacrjournals.org/).

Corresponding Author: David J. Waxman, Department of Biology, Boston University, 5 Cummington Street, Boston, MA 02215. Fax: 617-353-7404. E-mail: djw@bu.edu

but are not optimal for vascular normalization. Supporting this possibility, increases in chemotherapeutic drug uptake are seen in some tumor models at low but not standard doses of the antiangiogenic agent sunitinib (21, 22), and improved antitumor responses are reported when bevacizumab is given to patients at low dose, but not high dose, in combination with conventional chemotherapy (23). An alternative reason why certain VEGF receptor RTKIs might not induce normalization may due to their coinhibition of PDGFR-β, which promotes the close association between pericytes and endothelial cells that characterizes normal blood vessels (24), thereby destabilizing tumor blood vessels in a way that interferes with tumor vascular normalization induced by VEGF deprivation. These two possibilities are examined in the present study, where the impact of antiangiogenesis on tumor drug uptake is investigated over a range of doses for both axitinib and AG-028262, an antiangiogenic RTKI whose specificity for VEGFR-2 as compared with PDGFR-β is approximately 50-fold greater than that of axitinib (25).

As blood flow to the tumor decreases in response to antiangiogenesis, blood flow out of the tumor may also decrease. This could potentially increase the retention of therapeutic agents in tumors. Furthermore, for drugs that successfully extravasate into the tumor extracellular matrix, a decrease in tumor interstitial fluid pressure following antiangiogenesis treatment may slow the leakage of drugs from the tumor periphery to the peritumoral space and could also lead to longer tumor drug retention. However, the inhibition of VEGF signaling reduces the permeability of blood vessels and can adversely affect the extravasation of drugs after they are delivered into the tumor through blood circulation (26). Thus, even if antiangiogenesis increase the retention of therapeutic agents in tumor vasculature, it is uncertain whether this can be translated into increased interstitial drug concentration and higher tumor cell drug exposure. These questions are presently investigated in a 9L gliosarcoma model that expresses cytochrome P450 2B11, which converts the anticancer prodrug CPA to its active, 4-hydroxy metabolite (27). Our findings demonstrate that pretreatment of P450 2B11–expressing tumors with angiogenesis inhibitors significantly increases tumor retention of CPA, as well as 4-OH-CPA, following intratumoral CPA delivery, leading to increases in tumor cell apoptosis and antitumor activity. Furthermore, we show that for a prodrug that can be administered systemically and activated intratumorally, as exemplified by CPA, the decrease in tumor drug uptake following angiogenesis inhibition can be fully reversed by the tumor drug retention effect induced by the same antiangiogenesis treatment.

Materials and Methods

Additional details on chemicals and analytical procedures, including drug treatments, 4-OH-CPA and CPA analysis, pharmacokinetic data analysis, endothelial cell chemosensitivity to 4-OH-CPA, and analysis of CPA-induced apoptosis are provided in Supplementary Materials

Tumor cell lines and xenograft models

9L rat gliosarcoma cells infected with a retroviral vector encoding P450 2B11 in combination with P450 reductase (9L/ 2B11 cells), and 9L tumor cells infected with the empty retroviral vector pBabe (9L cells) were described previously (28). Cells were grown in DMEM culture medium containing 10% FBS at 37°C in a humidified, 5% CO_2 atmosphere. Immune-deficient male Fox Chase ICR *scid* mice were purchased from Taconic, Inc. and housed in the Boston University Laboratory of Animal Care Facility in accordance with approved protocols and federal guidelines. Autoclaved cages containing food and water were changed once a week. Mouse body weight was monitored every 3 to 4 days. On the day of tumor cell inoculation, 9L or 9L/2B11 cells at 70% to 80% confluence were trypsinized and resuspended in FBS-free DMEM medium. Cells (4×10^6) in a volume of 0.2 mL were injected subcutaneously (s.c.) into each flank of a 6-week-old male *scid* mouse. Tumor sizes were measured every 3 to 4 days using digital calipers (VWR International) and volumes were calculated as $(3.14/6) \times (L \times W)^{3/2}$.

Tumor growth delay study

Mice bearing bilateral 9L/2B11 tumors were randomized into five groups on the day of initial drug treatment, when the average tumor volume reached 800 to 900 mm^3 (5–8 mice per group), and treated as follows: (i) vehicle injection [5 μL per g body weight, i.p., once a day (sid) for 4 days], followed by 120 μL PBS sid for 2 days, administered at 3 intratumoral injection sites per tumor at 20 μL per injection and 2 tumors/ mouse beginning 24 hours after the last vehicle injection; (ii) axitinib (25 mg/kg body weight, i.p., sid for 4 days); (iii) CPA [150 mg CPA/kg body weight in a total vol of 120 μL, administered at 3 intratumoral (i.t.) injection sites per tumor at ~20 μL per injection site and 2 tumors/mouse], sid for 2 days; (iv) CPA, followed by axitinib given 24 hours after the second CPA injection; and (v) axitinib, followed by CPA given 24 hour after the fourth axitinib injection. For groups (i) and (ii), the mice were terminated when the tumor volume reached the limit set by institutional guidelines. For groups (iii), (iv), and (v), a second drug treatment cycle was initiated on day 21, as shown in Figure 6, below, after which the mice were maintained drug-free. Tumor volume and mouse body weight were monitored throughout the study.

Statistical analysis

Results are expressed as mean ± SE based on the indicated number of tumors or tissue samples per group. Statistical significance of differences was assessed by 2-tailed Student's *t* test using GraphPad Prism software, and is indicated by *, $P < 0.05$; **, $P < 0.01$; and ***, $P < 0.001$. All drug-treated samples were compared with controls, unless indicated otherwise.

Results

VEGFR-selective inhibitors suppress 9L tumor uptake of CPA and 4-OH-CPA without vascular normalization

The anticancer prodrug CPA is activated by hepatic P450 enzymes and then delivered to the tumor via the bloodstream (29). Axitinib treatment for 4 days (25 mg/kg/day, i.p.) significantly reduced the number of blood vessels in 9L tumors grown s.c. in *scid* mice (Fig. 1A), consistent with our earlier

Figure 1. Axitinib and AG-028262 inhibit tumor uptake of CPA and 4-OH-CPA — *Scid* mice bearing s.c. 9L tumor xenografts with no pretreatment or pretreated with axitinib (25 mg/kg, i.p., sid for 4 days) were given a single i.p. injection of CPA (140 mg/kg). A, immunohistochemcial staining of CD31-positive blood vessels in 9L tumors before and after axitinib treatment. Intratumoral CPA (B) and 4-OH-CPA (C) concentrations were assayed 6 or 15 minutes after CPA treatment. Mean ± SE, $n = 6$ tumors per time point. D, 4-OH-CPA in 9L tumors treated with axitinib (2–25 mg/kg, p.o., bid), or AG-028262 (3–40 mg/kg, p.o., bid) for 4 days were assayed in tumors excised 15 minutes after i.p. injection of CPA. Numbers along *x*-axis indicate doses of axitinib or AG-028262 for each group in mg/kg. Mean ± SE, $n = 4$ to 6 tumors per group. *, $P < 0.05$; **, $P < 0.01$; ***, $P < 0.001$ compared with controls.
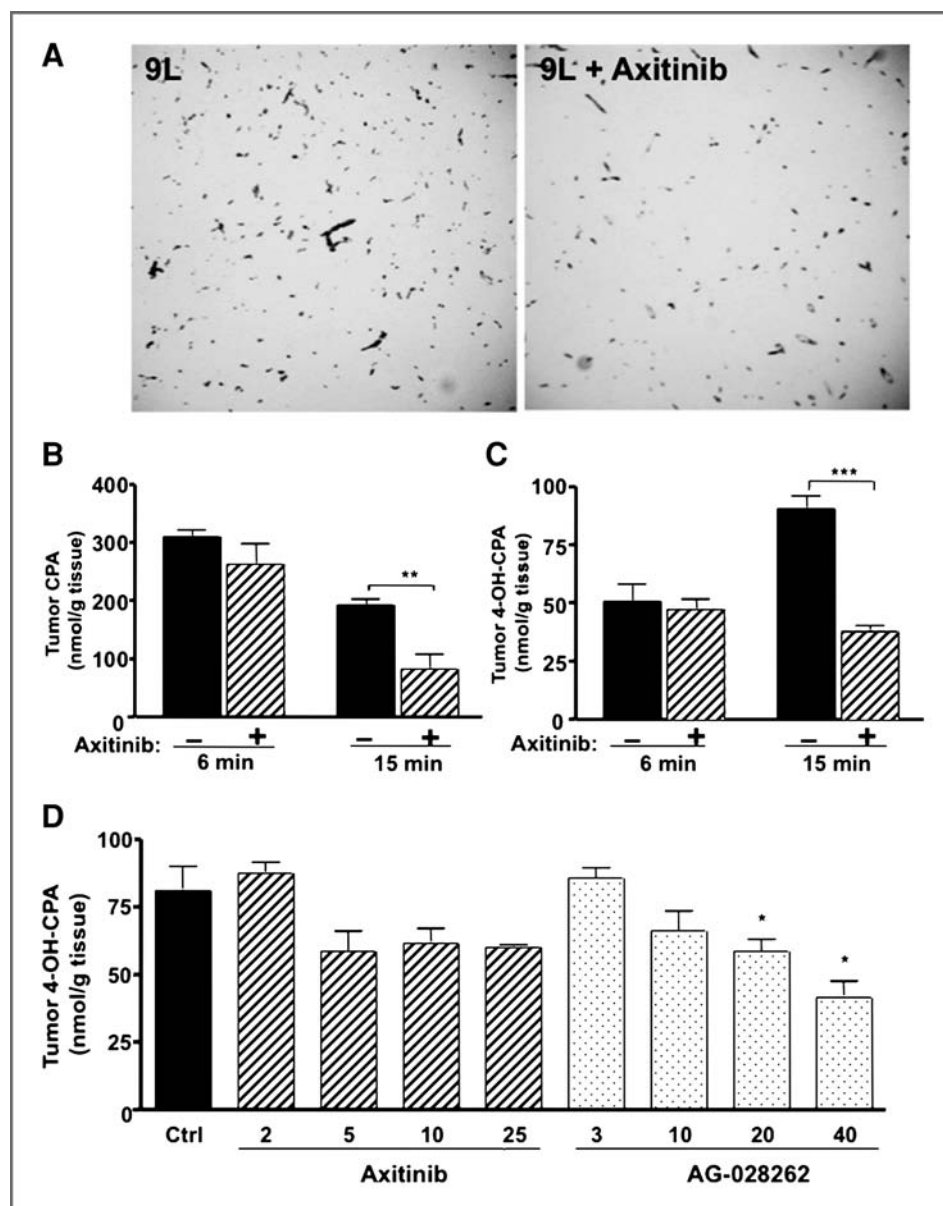
findings (14). Axitinib also decreased tumor uptake of CPA and of liver-derived 4-OH-CPA when assayed at the T_{max}, 15 minutes after i.p. injection of CPA (Fig 1B and C), indicating that axitinib suppresses tumor vascular patency, in agreement with earlier studies (14). To ascertain whether lower doses of axitinib might induce functional normalization of tumor blood vessels leading to an increase in tumor drug uptake, mice were treated with axitinib at doses ranging from 2 to 25 mg/kg [p.o., twice a day (bid)]. No axitinib-dependent increase in tumor uptake of 4-OH-CPA was seen at any of the doses tested. A dose of 2 mg/kg axitinib was without effect, whereas 5 mg/kg axitinib resulted in a maximal reduction in the intratumoral 4-OH-CPA concentration (Fig. 1D). Next, we investigated whether an increase in tumor vascular patency and drug uptake could be achieved using AG-208262, a more selective VEGFR-2 RTKI than axitinib (25). AG-028262 induced a progressive, dose-dependent decrease in intratumoral 4-OH-CPA over the full dose range tested (Fig. 1D). At 40 mg/kg, AG-208262 suppressed tumor 4-OH-CPA level by 48%, consistent with its strong antiangiogenic activity. Similar decreases in tumor uptake of CPA (Supplementary Fig. S1) and 4-OH-CPA (30) were seen in PC-3 tumors pretreated with axitinib at 25 mg/kg/day for times ranging from 0.5 to 6 days. Thus, VEGFR inhibition by either axitinib or AG-208262 is not associated with functional normalization of the tumor vasculature.

Antiangiogenesis increases exposure of 9L/2B11 tumors to CPA and 4-OH-CPA by increasing drug retention

Next, we investigated whether antiangiogenic drugs might be used to increase intratumoral drug retention. CPA was

Ma et al.

injected intratumorally into 9L/2B11 tumors, where CYP2B11, a cytochrome P450 enzyme, catalyzes intratumoral metabolism of CPA to its active metabolite, 4-OH-CPA. CPA that exits the tumor intact can be converted by liver P450 enzymes to 4-OH-CPA, a portion of which may then reenter the tumor (27). Five minutes after CPA injection, intratumoral CPA levels were 580 μmol/L in untreated tumors as compared with 1,840 μmol/L in axitinib-pretreated tumors (Fig. 2A). However, the initial tumor level of 4-OH-CPA was not significantly higher in the axitinib-pretreated tumors (Fig. 2B), indicating that axitinib does not increase the intrinsic rate of intratumoral CPA 4-hydroxylation, despite the 3.2-fold increase in initial intratumoral CPA concentration. This finding can be explained by CYP2B11 being already saturated at the concentration of 580 μmol/L CPA that is reached when CPA is injected i.t. without prior axitinib treatment [c.f., K_m (CPA) = 70 μmol/L in 9L/2B11 cells; ref 28]. As the intratumoral CPA levels declined with time due to a combination of drug efflux and intratumoral conversion to 4-OH-CPA, we observed an increase in overall intratumoral 4-OH-CPA exposure with axitinib treatment (Fig. 2B). Total intratumoral exposure to CPA, and 4-OH-CPA was 76% to 77% higher in axitinib-pretreated mice, as indicated by area under the curve (AUC; Table 1). This finding is consistent with axitinib slowing drug efflux from the tumors. After 30 minutes, intratumoral 4-OH-CPA levels declined both with and without axitinib-pretreatment, reflecting depletion of the intratumoral pool of CPA available for metabolism to 4-OH-CPA. The C_{max} of tumor exposure to 4-OH-CPA was also increased with axitinib pretreatment, by 42% (Table 1B). CPA and 4-OH-CPA levels were substantially lower in plasma and liver than in the tumor (Fig. 2C–F), as is expected for an intratumoral route of drug delivery. Moreover, at the 5-minute time point, plasma and liver 4-OH-CPA levels were significantly lower in axitinib-pretreated mice than in controls ($P < 0.05$), indicating that the greater retention of CPA and 4-OH-CPA by the axitinib-pretreated tumor renders CPA less available for hepatic metabolism and also reduces the efflux of tumor-derived 4-OH-CPA during this initial time period. By 30 minutes, however, plasma and liver levels of CPA and 4-OH-CPA were higher in the axitinib-pretreated mice, reflecting the delay in drug release from the tumors.

To confirm the role of intratumoral P450 metabolism in the observed retention of 4-OH-CPA, we used mice bearing wild-type 9L tumors to investigate the impact of axitinib pretreatment on the intratumoral pharmacokinetics of CPA and 4-OH-following i.t. CPA injection. Wild-type 9L tumors do not express significant levels of P450 enzymes and cannot metabolize CPA to 4-OH-CPA. As anticipated, we observed higher levels of intratumoral CPA in the axitinib-pretreated tumors at both 6 and 15 minutes, reflecting increased tumor drug retention (Fig. 2G), however, intratumoral 4-OH-CPA levels were lower through 30 minutes, reflecting the inhibition of tumor uptake of 4-OH-CPA formed in the liver (Fig. 2H).

Two other antiangiogenic drugs, AG-028262 and SU5416, were investigated for their effects on intratumoral drug retention in mice bearing 9L/2B11 tumors (Fig. 3). Four days of pretreatment with AG-028262 or SU5416 had no significant effect on intratumoral CPA or 4-OH-CPA levels 15 minutes

after intratumoral CPA injection, although a trend of increasing drug retention was apparent for CPA (Fig. 3A). However, 30 minutes after CPA injection, when intratumoral CPA concentrations decreased well below the K_m for metabolism by CYP2B11 (c.f.; Fig. 2A), both antiangiogenic drugs significantly increased intratumoral 4-OH-CPA compared with controls ($P < 0.05$; Fig. 3B). Thus, prolonged tumor drug retention may represent a common response to antiangiogenesis treatments involving these RTKIs.

Although axitinib decreased tumor levels of both CPA and 4-OH-CPA in mice bearing wild-type 9L tumors following i.p. CPA administration (Fig. 4A and B, left set of bars; also see Fig. 1B and C; refs. 11, 14), axitinib effected no such decrease in tumor 4-OH-CPA levels in mice bearing 9L/2B11 tumors either 15 or 30 minutes after i.p. injection of CPA (Fig. 4B). This can be explained by the increased retention of CPA that enters the axitinib-pretreated tumors, which makes CPA more available for metabolism by the tumor cell-expressed P450 2B11 enzyme, and by the increased retention of tumor cell-derived 4-OH-CPA. This increased retention of CPA and 4-OH-CPA in part compensates for the decreased tumor uptake of 4-OH-CPA that is formed in the liver. Thus, antiangiogenesis not only increases the exposure of tumor cells to drugs delivered intratumorally, but can also increase intratumoral metabolism, and exposure, to the activated form of a prodrug that is administered systemically.

In control experiments, we observed that the CPA 4-hydroxylase activity of 9L/2B11 tumor-derived microsomes was not altered by axitinib pretreatment (Supplementary Fig. S2). Hepatic cytochrome P450-catalyzed CPA 4-hydroxylation is also unaffected by axitinib treatment (14). Thus, the increase in intratumoral concentration of 4-OH-CPA seen following axitinib treatment cannot be explained by an increase in the intrinsic CPA 4-hydroxylase activity of either the liver or tumor.

Axitinib enhances CPA-induced tumor cell apoptosis

The impact of the enhanced drug retention following axitinib treatment on tumor cell apoptosis was investigated by measuring caspase activity in tumor samples excised 24 hours after the last drug treatment. Basal 9L/2B11 tumor caspase activity was unaffected by axitinib treatment (Fig. 5A). Intratumoral administration of CPA (50 mg/kg, 2 injections 24 hours apart) significantly increased caspase activity. However, the highest caspase activity was observed when mice bearing the intratumoral CPA-treated 9L/2B11 tumors were pretreated with axitinib (Fig. 5A). Thus, the prolonged exposure of tumor cells to 4-OH-CPA translates into a significant increase in tumor cell apoptosis. Axitinib had no effect on the intrinsic sensitivity of endothelial cells to activated CPA, as determined using cultured HUVEC cells (Fig. 5B).

Axitinib enhances the antitumor activity of intratumoral CPA injection

The therapeutic impact of axitinib-enhanced tumor drug retention was investigated in a tumor growth delay study. Four days of axitinib treatment resulted in a transient ($\sim$3 day) delay in 9L/2B11 tumor growth, whereas maximum

Figure 2. Impact of axitinib on CPA and 4-OH-CPA pharmacokinetics following intratumoral CPA injection. *Scid* mice bearing s.c. 9L/2B11 tumor xenografts without (solid lines) or with axitinib pretreatment (dashed lines; 25 mg/kg, i.p., sid for 4-days) were given a single i.t. injection of CPA at 50 mg/kg at $t = 0$ minutes. CPA and 4-OH-CPA levels were determined in 9L/2B11 tumors (A, B), plasma (C, D) and liver (E, F) 5–240 minutes after CPA administration. CPA (G) and 4-OH-CPA (H) were also determined in 9L tumors grown s.c. in *scid* mice following i.t. CPA injection, without or with axitinib pretreatment, as in A and B. Mean $\pm$ SE, $n = 3$ mice (6 tumors) per time point. *, $P < 0.05$; **, $P < 0.01$; ***, $P < 0.001$ for axitinib pretreated compared with controls.
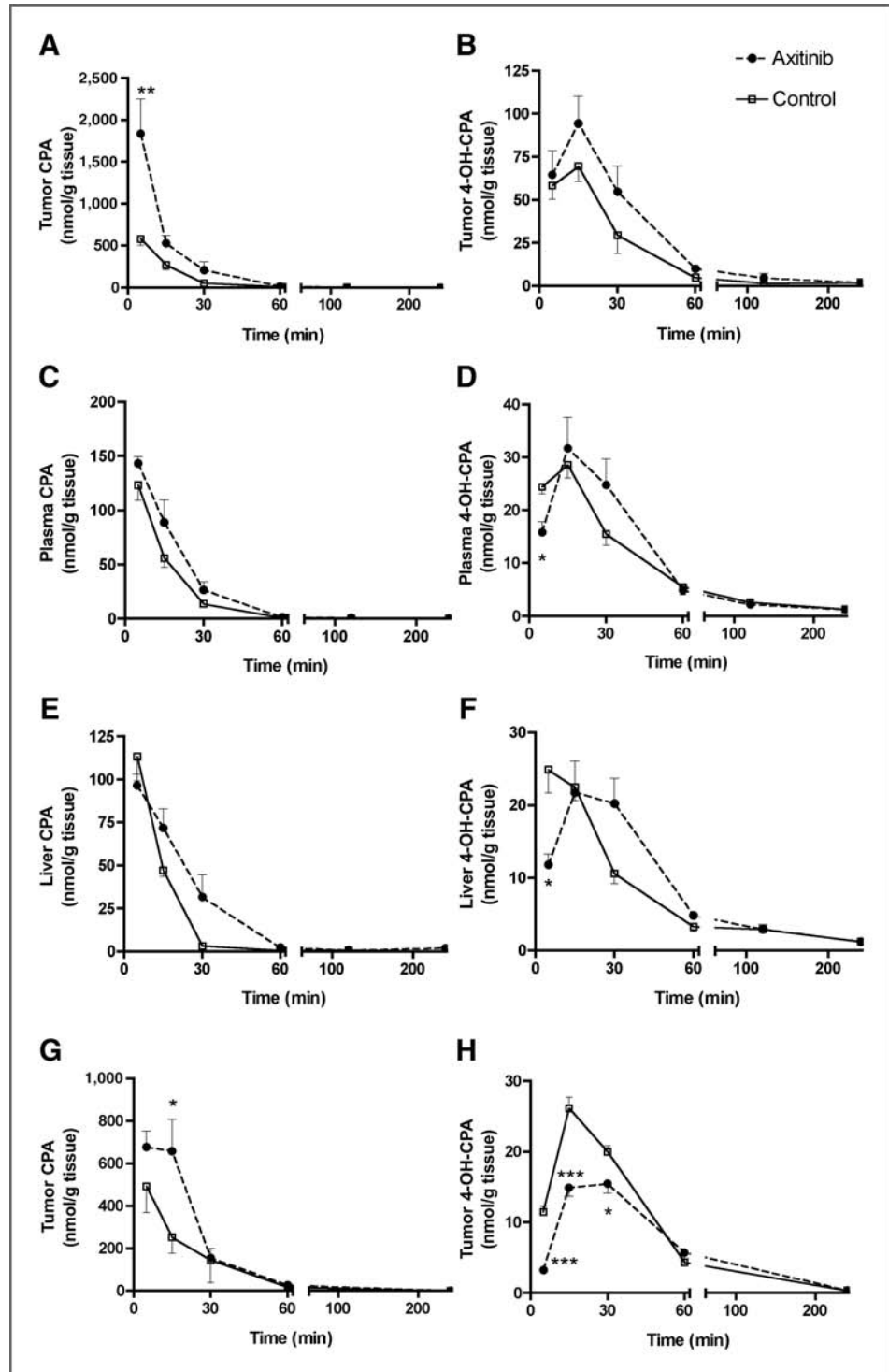
tolerated dose-scheduled CPA (2 intratumoral CPA administration spaced 24 hours apart) resulted in substantially longer tumor growth delay (Fig. 6A; Table 2). However, robust tumor growth eventually resumed, even when each cycle of CPA treatment was followed by axitinib treatment (CPA/axitinib schedule). In contrast, when axitinib was administered for 4 days prior to intratumoral CPA injection (axitinib/CPA schedule), i.e., conditions under which axitinib increases drug retention and intratumoral exposure to 4-OH-CPA, tumor growth stasis was sustained for at least 22 days after the last

Table 1. Axitinib pretreatment increases tumor retention of CPA and 4-OH-CPA

		$AUC_{0\to\infty}$ nmol/g-min	C_{max} nmol/g	T_{max} min	$t_{1/2}$ min
A. CPA pharmacokinetics					
Tumor	Untreated	364 ± 46	$5{,}040 \pm 419$	0.5 ± 0	10 ± 1
	Axitinib	642 ± 79^{a}	$5{,}405 \pm 449$	0.5 ± 0	13 ± 3
Plasma	Untreated	33 ± 4	123 ± 14	5 ± 0	24 ± 1
	Axitinib	48 ± 9	143 ± 6	5 ± 0	24 ± 0
Liver	Untreated	27 ± 3	113 ± 14	5 ± 0	30 ± 2
	Axitinib	45 ± 11	96 ± 7	5 ± 0	35 ± 5
B. 4-OH-CPA pharmacokinetics					
Tumor	Untreated	48 ± 4	84 ± 6	12 ± 2	36 ± 2
	Axitinib	85 ± 6^{b}	119 ± 9^{b}	16 ± 3	34 ± 2
Plasma	Untreated	24 ± 4	29 ± 2	15 ± 0	42 ± 7
	Axitinib	26 ± 4	32 ± 6	15 ± 0	37 ± 9
Liver	Untreated	21 ± 4	25 ± 3	8 ± 3	30 ± 1
	Axitinib	24 ± 3	22 ± 4	20 ± 5	48 ± 11

Note: Levels of CPA (A) or 4-OH-CPA (B) in 9L/2B11 tumor, plasma, and liver were measured from 5 to 240 minutes following a single i.t. injection of CPA (50 mg/kg) based on Figure 2. Values are expressed as mean $\pm$ SE. [a], $P < 0.05$; [b], $P < 0.01$, compared with untreated controls, with $n = 3$ mice and $n = 6$ tumors per group.

cycle of drug treatment (Fig. 6A; $P < 0.05$, 1-way ANOVA, day 0 to day 49 for axitinib/CPA schedule vs. CPA/axitinib schedule). Similar body weight profiles were observed for the CPA monotherapy and for both axitinib-CPA schedules (Fig. 6B), indicating that no additional toxicities were associated with the axitinib/CPA schedule. A small body weight loss occurred after each CPA treatment, as is typical for this cytotoxic drug. Thus, the extended drug retention associated with neoadjuvant axitinib treatment significantly enhances CPA antitumor activity.

Discussion

In the present study, we investigated how VEGF receptor-targeted antiangiogenic agents modulate chemotherapeutic drug delivery and drug retention by the tumor. Antiangiogenesis was found to decrease tumor uptake of the anticancer prodrug CPA and its active metabolite, 4-OH-CPA, consistent with the established requirement for a functional tumor vasculature and blood flow for effective drug delivery. However, in mice bearing tumors that express the CPA-activating cytochrome P450 enzyme CYP2B11, neoadjuvant axitininb treatment significantly increased the AUC of intratumoral 4-OH-CPA exposure following intratumoral CPA administration, leading to an increase in tumor cell apoptosis and a major increase in antitumor activity, as seen in tumor growth delay studies. Increased tumor drug retention was also seen with two other antiangiogenic agents, indicating that this effect is a general response to tumor antiangiogenesis. Importantly, the increases in therapeutic activity were achieved despite the transient nature of the tumor drug retention effect of neoadjuvant axitinib treatment, and they cannot be explained by an increase in tumor cell or endothelial cell chemosensitivity following axitinib treatment (14). Further-

more, no increase in antitumor activity was seen when CPA treatment preceded axitinib administration, consistent with the proposed mechanism for the improved therapeutic response, namely, antiangiogenesis-dependent drug retention leading to increased tumor cell exposure to 4-OH-CPA. Finally, when CPA was administered systemically and activated intratumorally, the decreases in tumor uptake of both CPA and 4-OH-CPA due to antiangiogenesis were counter-balanced, and fully compensated for, by antiangiogenesis-induced drug retention. Thus, when a tumor-activated prodrug is administered systemically, antiangiogenesis-induced drug retention can counteract the decrease in drug uptake while at the same time retaining the therapeutic benefits of antiangiogenesis-induced tumor cell starvation.
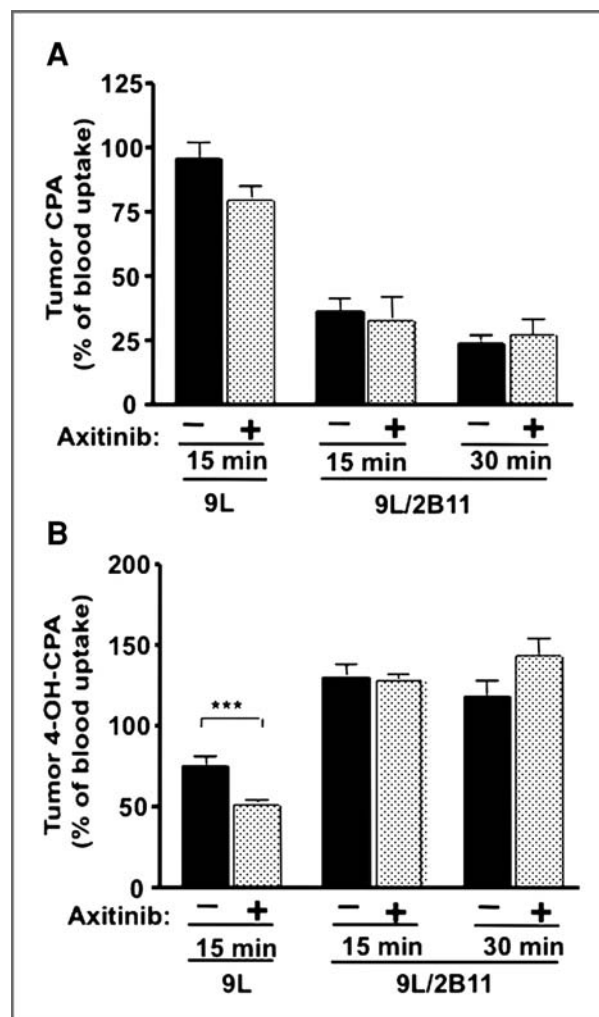
Antiangiogenesis induces morphological normalization of the tumor vasculature, which involves pruning of immature blood vessels, a decrease in blood vessel tortuosity and dilation, and a closer association between pericytes and tumor endothelial cells (12). This can lead to functional improvements, as shown by the increases in tumor vascular patency and drug uptake and decreases in tumor hypoxia reported in preclinical studies with several antiangiogenic agents (31). However, these effects are short lived and they disappear with continued antiangiogenic drug treatment (32, 33). Moreover, for axitinib (15, 34) and certain other antiangiogenic drugs (17, 35, 36), although morphological normalization of the tumor vasculature and improved functionality of individual blood vessels may occur, overall tumor vascular patency and capacity for drug uptake actually decrease. Presently, we investigated the hypothesis that tumor blood vessel normalization leading to increased drug uptake can be achieved by reducing the dose of the antiangiogenic RTKI; however, we obtained no evidence for such functional normalization of tumor
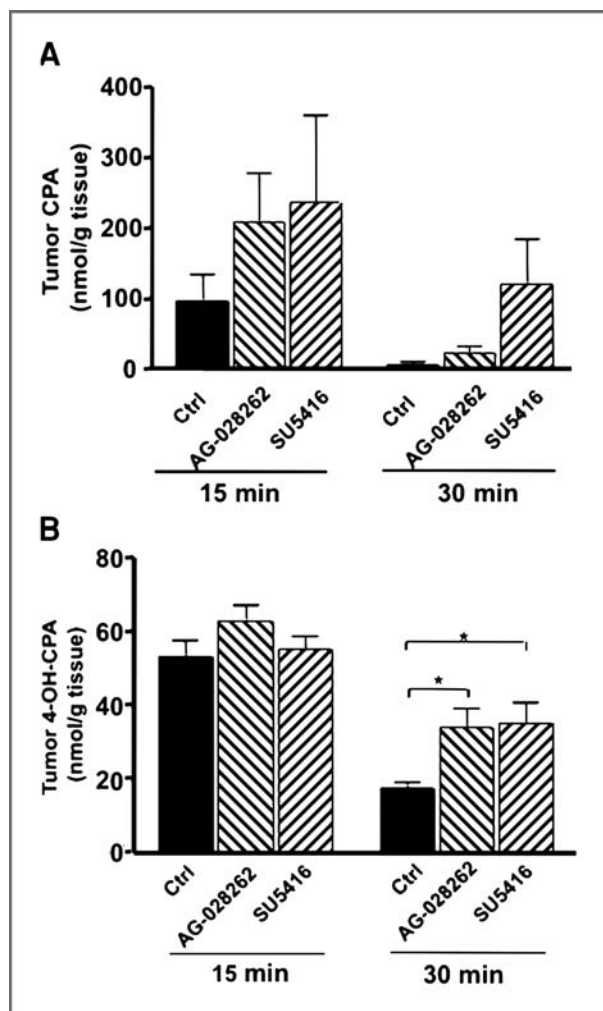
Figure 3. Impact of other antiangiogenic drugs on tumor drug retention following intratumoral CPA administration. *Scid* mice bearing s.c. 9L/2B11 tumors were pretreated for 4 days with AG-028262 (40 mg/kg, p.o., bid) or SU5416 (25 mg/kg, i.p., sid), followed by i.t. injection of CPA at 50 mg/kg on day 5. Tumor levels of CPA (A) and 4-OH-CPA (B) were determined 15 and 30 minutes later. Mean ± SE, $n = 5$ to 6 tumors per group. *, $P < 0.05$ compared with vehicle controls (Ctrl).

Figure 4. Impact of axitinib on tumor drug retention following systemic CPA administration. *Scid* mice bearing s.c. 9L or 9L/2B11 tumors were pretreated for 4 days with vehicle or axitinib (25 mg/kg/day, i.p., sid), followed by i.p. injection of CPA at 50 mg/kg on day 5. Tumor levels of CPA (A) and 4-OH-CPA (B) were determined 15 and 30 minutes later. Mean ± SE, $n = 6$ to 12 tumors per group. ***, $P < 0.001$ compared with vehicle controls.

vasculature over a more than 10-fold dose range of either axitinib or AG-028262. Moreover, our studies with AG-028262 rule out cross-inhibition with PDGFR-β as a reason for the absence of normalization, given the high selectivity of this RTKI for VEGFR inhibition (25).

The absence of tumor vessel normalization in these preclinical studies is consistent with the limited therapeutic benefit reported in several phase III clinical trials combining antiangiogenic agents with conventional chemotherapies (8–10). The poor performance of these combination therapies indicates a need to consider new approaches, such as the antiangiogenesis-induced tumor drug retention approach reported here. In particular, for cytotoxic agents that can be delivered or activated intratumorally, persistent angiogenesis inhibition may further increase drug retention and therapeutic activity. Other approaches may include optimization of the timing and sequen-

cing of antiangiogenic agents given in combination with cytotoxic drugs, as discussed elsewhere (11). For antiangiogenic agents that show limited activity in a monotherapy setting and that transiently induce functional normalization of the tumor vasculature, intermittent neoadjuvant antiangiogenesis prior to each cycle of cytotoxic drug administration may increase tumor drug uptake. However, for combination therapies that include potent antiangiogenic drugs that do not induce tumor vascular normalization, a brief period of antiangiogenic drug treatment at a reduced dose, or temporary dilation of tumor blood vessels (37) prior to chemotherapy administration may be required to minimize the negative impact of angiogenesis inhibition on tumor drug uptake.

Tumor uptake of 4-OH-CPA, the active metabolite of CPA, was inhibited by axitinib and AG-028262, which reduce tumor
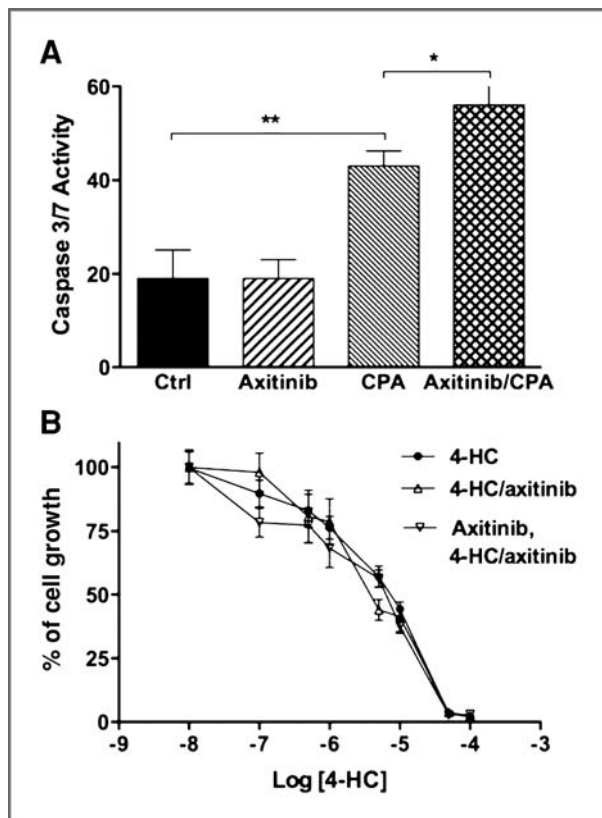
Figure 5. Effects of axitinib on CPA-induced tumor cell apoptosis and endothelial cell chemosensitivity. A, *Scid* mice bearing s.c. 9L/2B11 tumor xenografts pretreated for 4 days with vehicle or axitinib (25 mg/kg, i.p., sid) were injected with phosphate-buffered-saline (control) or CPA (50 mg/kg, i.t., 2 injections 24 hours apart). Tumor cell apoptosis was determined 24 hours after the last drug treatment by measuring caspase activity in the absence or in the presence of the caspase inhibitor casputin. Mean $\pm$ SE, $n = 6$ tumors per treatment. *, $P < 0.05$; **, $P < 0.01$ for the comparisons indicated. B, cultured HUVEC cells were treated with chemically activated CPA, 4-HC, alone or in combination with axitinib. The effect of drug treatment on final cell number (cell proliferation) was determined by crystal violet staining. Mean $\pm$ SE, $n = 3$ per data point.

blood perfusion and total vascular volume and decrease the number of patent tumor blood vessels (16, 34). These responses not only decrease chemotherapeutic drug uptake, but as shown here, they also decrease the rate at which drug molecules exit from the tumor, resulting in prolonged drug retention and increased tumor drug exposure. In the case of 9L/2B11 tumors given a single intratumoral injection of CPA, axitinib increased tumor cell exposure to CPA, and to 4-OH-CPA almost 2-fold, as judged by AUC values. As axitinib also decreases tumor uptake of liver-derived 4-OH-CPA, with no change in the intrinsic CPA 4-hydroxylase activity of 9L/2B11 tumors, these increases in tumor drug exposure likely underestimate the extent to which axitinib inhibits tumor efflux of 4-OH-CPA *per se*. Indeed, axitinib decreased the initial rate of tumor efflux of CPA by approximately 3-fold, as judged from the 3.2-fold higher residual intratumoral CPA concentration determined 5 minutes after drug injection (1,840 vs. 580 μmol/L). P450 2B11 has a K_m (CPA) of 70 μmol/L in 9L/2B11 cells (28), indicating that tumor
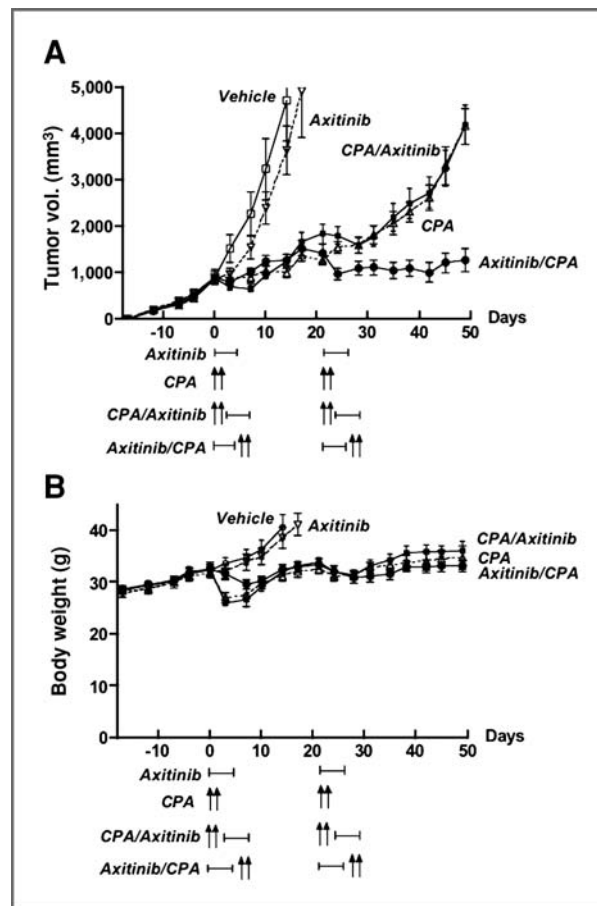
Figure 6. Impact of neoadjuvant axitinib treatment on antitumor activity of intratumoral CPA treatment. 9L/2B11 tumors were implanted s.c. in *scid* mice. Arrows along the *x*-axis indicate the days on which CPA was administered (150 mg/kg, 2 i.t. injections 24 hours apart, drug treatment cycle repeated beginning on day 21) and the horizontal lines below the *x*-axis indicate the time period of axitinib treatment (25 mg/kg, i.p., sid). Drug treatment was initiated on day 0, when the average tumor size of each group reached 800 to 900 mm³. A, antitumor activity of intratumoral CPA injection was substantially prolonged in mice given 4 daily axitinib injections prior to CPA treatment (Axitinib/CPA schedule) compared with intratumoral CPA treatment followed by axitinib (CPA/Axitinib schedule) or intratumoral CPA treatment alone. Axitinib treatment alone resulted in only a 3 day growth delay. Also see Table 2. B, impact of axitinib and CPA treatment schedule on body weight for the same mice shown in panel A. No additional body weight loss was induced by the combination drug treatments compared with CPA treated tumor-bearing mice. Mean $\pm$ SE, $n = 10$ to 16 tumors per group.

cell capacity for CPA 4-hydroxylation (drug activation) is saturated during the initial 15 to 30 minutes period after intratumoral CPA injection. Thus, the increase in tumor cell apoptosis and therapeutic activity seen in our experiments may very well underestimate the drug retention effect of antiangiogenesis. A larger increase in therapeutic activity can therefore be anticipated for other, direct-acting drugs, or in the case of CPA, for tumors that express a prodrug activation enzyme less efficient than CYP2B11.

There are several important limitations of the antiangiogenesis-induced tumor drug retention effect reported here.

Table 2. Effect of drug schedule on tumor doubling time.

	Tumor doubling time (days)	
Vehicle (10)	5.1 ± 0.5	
Axitinib (10)	8.0 ± 0.4	$P = 0.0003$
CPA (10)	28.4 ± 3.6	$P < 0.0001$
CPA/Axitinib (16)	21.3 ± 2.16	$P < 0.0001$
Axitinib/CPA (14)	$> 49^a$	$P < 0.0001$

NOTE: Data shown are based on data presented in Fig. 6. Tumor sizes were measured every 3–4 days using digital calipers and volumes calculated as $(3.14/6) \times (L \times W)^{3/2}$. Values are expressed as mean $\pm$ SE. The number of individual tumors included in each treatment group is shown in parentheses. Statistical significance of differences was assessed by comparing each drug treatment group with vehicle control using 2-tailed Student's t test.

[a]Tumor growth was blocked after initiation of drug treatment (see Fig. 6) and 10 of 14 tumors never doubled in volume.

First, antiangiogenesis slows down but does not completely block tumor drug efflux. Moreover, drug retention becomes less prominent when baseline intratumoral drug concentrations are very low. Presumably, the residual efflux capability of the tumor vasculature is sufficient for export when the chemotherapeutic drug is present at low concentrations. Most important, the same antiangiogenic mechanisms that increase tumor drug retention also decrease chemotherapeutic drug uptake by the tumor. Thus, to take advantage of the increase in tumor drug retention and translate it into a meaningful therapeutic benefit, it needs to be utilized in a way that overcomes or circumvents the associated decrease in drug uptake from systemic circulation. This can be achieved by combining neoadjuvant antiangiogenic treatment with direct delivery of a chemotherapeutic drug into target tissues. Although intratumoral drug delivery is not suitable for all solid tumors and may impose certain practical limitations, it has been used in the clinic for treatment of head and neck cancer, lung cancer, and breast cancer (38–40) and can also be used in cases where tumors are not amenable to resection or as an adjuvant following tumor resection (41, 42). The benefits of antiangiogenesis induced tumor drug retention can also be realized in combination therapies involving systemic administration of a tumor-activated prodrug. This approach was exemplified for the P450 prodrug CPA in mice bearing tumors that express CYP2B11, where the axitinib-dependent decrease in tumor uptake of CPA and 4-OH-CPA from systemic circulation was fully compensated by the increase in tumor retention of 4-OH-CPA generated intratumorally. This drug retention effect helps explain our earlier finding that maximal antitumor activity is achieved in mice bearing 9L/2B11 tumors when systemic CPA administration is preceded by axitinib treat-

ment (30). Finally, the potential limitations imposed by the subcutaneous tumor xenografts model used here should be noted. The tumor microenvironment can have a significant impact on angiogenesis (43), and malignant gliomas grown orthotopically may be more hypoxic and less highly vascularized than the subcutaneous 9L tumors used in our studies (14, 44). These differences in tumor microenvironment may impact drug uptake as well as the extent to which antiangiogenesis increases overall drug exposure via the drug retention effect described here.

The principle of antiangiogenesis-induced tumor drug retention presented here may be applied to systemic treatments based on other therapeutic agents that can be activated intratumorally, including other P450 prodrugs (29), prodrugs activated by other enzymes (45), and bioreductive drugs, which are activated within hypoxic tumor regions (46). Antiangiogenesis-induced tumor drug retention may also be extended to increase the retention of tumor cell replicating, oncolytic viral vectors (47) as well as tumor-targeted nanoparticles (48). As tumor-specific delivery of nanoparticles in part depends on the enhanced permeability and leakiness of the tumor vasculature (48), the net impact of antiangiogenesis on tumor vascular permeability and drug retention is uncertain and will require further study. Increased tumor drug retention can also be expected for agents that transiently normalize tumor vasculature, once they ultimately decrease tumor vascular patency with continued use, and for vascular disrupting agents, which induce an acute interruption of tumor blood perfusion (49). The latter possibility is supported by the increased tumor exposure to the alkylating agent melphalan following pretreatment with the vascular disruption agent 5,6-dimethylxanthenone-4-acetic acid (50), and by the increase in activity when doxorubicin was combined with the vascular disruption agent ICT2588, where maximal antitumor activity was achieved when doxorubicin was administered after the collapse of the tumor vasculature induced by ICT2558 (51).

In conclusion, antiangiogenesis-induced tumor drug retention is an intrinsic action of antiangiogenic drugs and can be applied to a variety of antiangiogenesis treatments. This drug retention effect was employed to significantly increase the therapeutic activity of CPA treatment in a 9L xenograft model, and similar benefits can be expected with other tumor types. An even more pronounced drug retention effect can be anticipated for chronic antiangiogenesis treatment, when the decrease in functional tumor vasculature becomes more substantial, and perhaps for vascular disrupting agents as well. These findings provide a novel perspective and insight into the complex pharmacokinetic and pharmacodynamic effects and interactions between antiangiogenic drugs and chemotherapeutic agents and may stimulate further research to take advantage of these findings in a way that may circumvent the decrease in drug uptake that is also intrinsic to antiangiogenic therapies. Finally, certain normal tissues are also sensitive to VEGF/VEGFR inhibition (25, 52), indicating that the vasculature in these tissues may also be targeted for antiangiogenesis-induced drug retention.

Disclosure of Potential Conflicts of Interests

Acknowledgemnts

Grant Support

References

1. Minchinton AI, Tannock IF. Drug penetration in solid tumours. Nat Rev Cancer 2006;6:583–92.
2. Moses MA, Brem H, Langer R. Advancing the field of drug delivery: taking aim at cancer. Cancer Cell 2003;4:337–41.
3. Sonveaux P. Provascular strategy: Targeting functional adaptations of mature blood vessels in tumors to selectively influence the tumor vascular reactivity and improve cancer treatment. Radiother Oncol 2008;86:300–13.
4. Hurwitz H, Fehrenbacher L, Novotny W, Cartwright T, Hainsworth J, Heim W, et al. Bevacizumab plus irinotecan, fluorouracil, and leucovorin for metastatic colorectal cancer. N Engl J Med 2004;350:2335–42.
5. Sandler A, Gray R, Perry MC, Brahmer J, Schiller JH, Dowlati A, et al. Paclitaxel-carboplatin alone or with bevacizumab for non-small-cell lung cancer. N Engl J Med 2006;355:2542–50.
6. Escudier B, Eisen T, Stadler WM, Szczylik C, Oudard S, Siebels M, et al. Sorafenib in advanced clear-cell renal-cell carcinoma. N Engl J Med 2007;356:125–34.
7. Motzer RJ, Hutson TE, Tomczak P, Michaelson MD, Bukowski RM, Rixe O, et al. Sunitinib versus interferon alfa in metastatic renal-cell carcinoma. N Engl J Med 2007;356:115–24.
8. Hauschild A, Agarwala SS, Trefzer U, Hogg D, Robert C, Hersey P, et al. Results of a phase III, randomized, placebo-controlled study of sorafenib in combination with carboplatin and paclitaxel as second-line treatment in patients with unresectable stage III or stage IV melanoma. J Clin Oncol 2009;27:2823–30.
9. Scagliotti G, Novello S, von Pawel J, Reck M, Pereira JR, Thomas M, et al. Phase III study of carboplatin and paclitaxel alone or with sorafenib in advanced non-small-cell lung cancer. J Clin Oncol 2010;28:1835–42.
10. Herbst RS, Sun Y, Eberhardt WE, Germonpré P, Saijo N, Zhou C, et al. Vandetanib plus docetaxel versus docetaxel as second-line treatment for patients with advanced non-small-cell lung cancer (ZODIAC):a double-blind, randomised, phase 3 trial. Lancet Oncol 2010;11:619–26.
11. Ma J, Waxman DJ. Combination of antiangiogenesis with chemotherapy for more effective cancer treatment. Mol Cancer Ther 2008;7:3670–84.
12. Jain RK. Normalization of tumor vasculature: an emerging concept in antiangiogenic therapy. Science 2005;307:58–62.
13. Hu-Lowe DD, Zou HY, Grazzini ML, Hallin ME, Wickman GR, Amundson K, et al. Nonclinical antiangiogenesis and antitumor activities of axitinib (AG-013736), an oral, potent, and selective inhibitor of vascular endothelial growth factor receptor tyrosine kinases 1, 2, 3. Clin Cancer Res 2008;14:7272–83.
14. Ma J, Waxman DJ. Modulation of the antitumor activity of metronomic cyclophosphamide by the angiogenesis inhibitor axitinib. Mol Cancer Ther 2008;7:79–89.
15. Nakahara T, Norberg SM, Shalinsky DR, Hu-Lowe DD, McDonald DM. Effect of inhibition of vascular endothelial growth factor signaling on distribution of extravasated antibodies in tumors. Cancer Res 2006;66:1434–45.
16. Fenton BM, Paoni SF. The addition of AG-013736 to fractionated radiation improves tumor response without functionally normalizing the tumor vasculature. Cancer Res 2007;67:9921–8.
17. Franco M, Man S, Chen L, Emmenegger U, Shaked Y, Cheung AM, et al. Targeted anti-vascular endothelial growth factor receptor-2 therapy leads to short-term and long-term impairment of vascular function and increase in tumor hypoxia. Cancer Res 2006;66:3639–48.
18. Ma J, Pulfer S, Li S, Chu J, Reed K, Gallo JM. Pharmacodynamic-mediated reduction of temozolomide tumor concentrations by the angiogenesis inhibitor TNP-470. Cancer Res 2001;61:5491–8.
19. Williams KJ, Telfer BA, Brave S, Kendrew J, Whittaker L, Stratford IJ, et al. ZD6474, a potent inhibitor of vascular endothelial growth factor signaling, combined with radiotherapy: schedule-dependent enhancement of antitumor activity. Clin Cancer Res 2004;10:8587–93.
20. Tailor TD, Hanna G, Yarmolenko PS, Dreher MR, Betof AS, Nixon AB, et al. Effect of pazopanib on tumor microenvironment and liposome delivery. Mol Cancer Ther 2010;9:1798–808.
21. Mendel DB, Laird AD, Xin X, Louie SG, Christensen JG, Li G, et al. *In vivo* antitumor activity of SU11248, a novel tyrosine kinase inhibitor targeting vascular endothelial growth factor and platelet-derived growth factor receptors: determination of a pharmacokinetic/pharmacodynamic relationship. Clin Cancer Res 2003;9:327–37.
22. Zhou Q, Guo P, Gallo JM. Impact of angiogenesis inhibition by sunitinib on tumor distribution of temozolomide. Clin Cancer Res 2008;14:1540–9.
23. Kabbinavar F, Hurwitz HI, Fehrenbacher L, Meropol NJ, Novotny WF, Lieberman G, et al. Phase II, randomized trial comparing bevacizumab plus fluorouracil (FU)/leucovorin (LV) with FU/LV alone in patients with metastatic colorectal cancer. J Clin Oncol 2003;21:60–5.
24. Abramsson A, Lindblom P, Betsholtz C. Endothelial and nonendothelial sources of PDGF-B regulate pericyte recruitment and influence vascular pattern formation in tumors. J Clin Invest 2003;112:1142–51.
25. Mancuso MR, Davis R, Norberg SM, O'Brien S, Sennino B, Nakahara T, et al. Rapid vascular regrowth in tumors after reversal of VEGF inhibition. J Clin Invest 2006;116:2610–21.
26. Dvorak HF. Vascular permeability factor/vascular endothelial growth factor: a critical cytokine in tumor angiogenesis and a potential target for diagnosis and therapy. J Clin Oncol 2002;20:4368–80.
27. Chen CS, Jounaidi Y, Su T, Waxman DJ. Enhancement of intratumoral cyclophosphamide pharmacokinetics and antitumor activity in a P450 2B11-based cancer gene therapy model. Cancer Gene Ther 2007;14:935–44.
28. Jounaidi Y, Chen C-S, Veal GJ, Waxman DJ. Enhanced antitumor activity of P450 prodrug-based gene therapy using the low Km cyclophosphamide 4-hydroxylase P450 2B11. Mol Cancer Ther 2006;5:541–55.
29. Roy P, Waxman DJ. Activation of oxazaphosphorines by cytochrome P450: application to gene-directed enzyme prodrug therapy for cancer. Toxicol In Vitro 2006;20:176–86.
30. Ma J, Waxman DJ. Dominant effect of antiangiogenesis in combination therapy involving cyclophosphamide and axitinib. Clin Cancer Res 2009;15:578–88.
31. Fukumura D, Duda DG, Munn LL, Jain RK. Tumor microvasculature and microenvironment: novel insights through intravital imaging in pre-clinical models. Microcirculation 2010;17:206–25.
32. Winkler F, Kozin SV, Tong RT, Chae SS, Booth MF, Garkavtsev I, et al. Kinetics of vascular normalization by VEGFR2 blockade governs brain tumor response to radiation: role of oxygenation, angiopoietin-1, and matrix metalloproteinases. Cancer Cell 2004;6:553–63.
33. Ansiaux R, Baudelet C, Jordan BF, Crokart N, Martinive P, DeWever J, et al. Mechanism of reoxygenation after antiangiogenic therapy using

SU5416 and its importance for guiding combined antitumor therapy. Cancer Res 2006;66:9698–704.

34. Inai T, Mancuso M, Hashizume H, Baffert F, Haskell A, Baluk P, et al. Inhibition of vascular endothelial growth factor (VEGF) signaling in cancer causes loss of endothelial fenestrations, regression of tumor vessels, and appearance of basement membrane ghosts. Am J Pathol 2004;165:35–52.

35. Riesterer O, Honer M, Jochum W, Oehler C, Ametamey S, Pruschy M. Ionizing radiation antagonizes tumor hypoxia induced by antiangiogenic treatment. Clin Cancer Res 2006;12:3518–24.

36. Claes A, Wesseling P, Jeuken J, Maass C, Heerschap A, Leenders WP. Antiangiogenic compounds interfere with chemotherapy of brain tumors due to vessel normalization. Mol Cancer Ther 2008;7:71–8.

37. Martinive P, De Wever J, Bouzin C, Baudelet C, Sonveaux P, Grégoire V, et al. Reversal of temporal and spatial heterogeneities in tumor perfusion identifies the tumor vascular tone as a tunable variable to improve drug delivery. Mol Cancer Ther 2006;5:1620–7.

38. Almond BA, Hadba AR, Freeman ST, Cuevas BJ, York AM, Detrisac CJ, et al. Efficacy of mitoxantrone-loaded albumin microspheres for intratumoral chemotherapy of breast cancer. J Control Release 2003;91:147–55.

39. Celikoglu F, Celikoglu SI, Goldberg EP. Bronchoscopic intratumoral chemotherapy of lung cancer. Lung Cancer 2008;61:1–12.

40. Duvillard C, Polycarpe E, Romanet P, Chauffert B. [Intratumoral chemotherapy:experimental data and applications to head and neck tumors]. Ann Otolaryngol Chir Cervicofac 2007;124:53–60.

41. Menei P, Jadaud E, Faisant N, Boisdron-Celle M, Michalak S, Fournier D, et al. Stereotaxic implantation of 5-fluorouracil-releasing microspheres in malignant glioma. Cancer 2004;100:405–10.

42. Vogl TJ, Muller PK, Mack MG, Straub R, Engelmann K, Neuhaus P. [Therapeutic options in non-resectable liver metastases. Percutaneous radiological interventions]. Chirurg 1999;70:133–40.

43. Fidler IJ. Angiogenic heterogeneity: regulation of neoplastic angiogenesis by the organ microenvironment. J Natl Cancer Inst 2001;93:1040–1.

44. Amberger-Murphy V. Hypoxia helps glioma to fight therapy. Curr Cancer Drug Targets 2009;9:381–90.

45. Portsmouth D, Hlavaty J, Renner M. Suicide genes for cancer therapy. Mol Aspects Med 2007;28:4–41.

46. Tredan O, Garbens AB, Lalani AS, Tannock IF. The hypoxia-activated ProDrug AQ4N penetrates deeply in tumor tissues and complements the limited distribution of mitoxantrone. Cancer Res 2009;69:940–7.

47. Libertini S, Iacuzzo I, Perruolo G, Scala S, Ieranò C, Franco R, et al. Bevacizumab increases viral distribution in human anaplastic thyroid carcinoma xenografts and enhances the effects of E1A-defective adenovirus dl922–947. Clin Cancer Res 2008;14:6505–14.

48. Byrne JD, Betancourt T, Brannon-Peppas L. Active targeting schemes for nanoparticle systems in cancer therapeutics. Adv Drug Deliv Rev 2008;60:1615–26.

49. Tozer GM, Kanthou C, Lewis G, Prise VE, Vojnovic B, Hill SA. Tumour vascular disrupting agents: combating treatment resistance. Br J Radiol 2008;81Spec No 1:S12–20.

50. Pruijn FB, van Daalen M, Holford NH, Wilson WR. Mechanisms of enhancement of the antitumour activity of melphalan by the tumour-blood-flow inhibitor 5,6-dimethylxanthenone-4-acetic acid. Cancer Chemother Pharmacol 1997;39:541–6.

51. Atkinson JM, Falconer RA, Edwards DR, Pennington CJ, Siller CS, Shnyder SD, et al. Development of a novel tumor-targeted vascular disrupting agent activated by membrane-type matrix metalloproteinases. Cancer Res 2010;70:6902–12.

52. Kamba T, Tam BY, Hashizume H, Haskell A, Sennino B, Mancuso MR, et al. VEGF-dependent plasticity of fenestrated capillaries in the normal adult microvasculature. Am J Physiol Heart Circ Physiol 2006;290:H560–76.

Cancer Research

AACR

Antiangiogenesis Enhances Intratumoral Drug Retention

Jie Ma, Chong-Sheng Chen, Todd Blute, et al.

Updated Version	Access the most recent version of this article at: doi:10.1158/0008-5472.CAN-10-3242
Supplementary Material	Access the most recent supplemental material at: http://cancerres.aacrjournals.org/content/suppl/2011/03/25/0008-5472.CAN-10-3242.DC1.html

Cited Articles	This article cites 52 articles, 29 of which you can access for free at: http://cancerres.aacrjournals.org/content/71/7/2675.full.html#ref-list-1

E-mail alerts	Sign up to receive free email-alerts related to this article or journal.
Reprints and Subscriptions	To order reprints of this article or to subscribe to the journal, contact the AACR Publications Department at pubs@aacr.org.
Permissions	To request permission to re-use all or part of this article, contact the AACR Publications Department at permissions@aacr.org.

Supplementary Materials and Methods

Chemicals - Axitinib and AG-028262 were obtained from Pfizer Global Research and Development (San Diego, CA). SU5416, CPA, NADPH and semicarbazide hydrochloride were purchased from Sigma-Aldrich Co. (St. Louis, MO). 4-hydroperoxycyclophosphamide (4-HC) was obtained from Dr. Ulf Niemeyer (Baxter Oncology GmbH, Frankfurt, Germany). Carboxymethyl cellulose (low viscosity) was purchased from MP Biomedicals (Solon, OH). Polyethylene glycol 400 (PEG-400) was purchased from Fisher Scientific (Hampton, NH). Caspase-Glo^{TM} 3/7 assay kit was purchasd from Promega (Madison, WI). Casputin, a selective inhibitor of caspase 3 and caspase 7, was purchased from BIOMOL International (Plymouth Meeting, PA). Protease inhibitor cocktail tablets were purchased from Roche Diagnostics (Mannheim, Germany). DMEM culture medium and fetal bovine serum (FBS) were purchased from Invitrogen (Carlsbad, CA). Human umbilical vein endothelial cells (HUVEC) and EGM-2 BulletKit culture medium were purchased from Cambrex Bio Science (East Rutherford, NJ).

Drug treatments and tissue 4-OH-CPA analysis – In one treatment schedule, mice bearing 9L tumors were randomized to different groups on the day of initial drug treatment when the average tumor volume reached ~500 mm^3. Axitinib (0.4 mg/ml to 5 mg/ml) and AG-028262 (0.2 mg/ml to 8 mg/ml) were suspended in 0.5% carboxymethyl cellulose and administered orally using a 20-gauge gavage feeding needle in a volume of 5 µl/g body weight every 12 hr for 4 days. Axitinib was administered at 2, 5, 10, or 25 mg/kg body weight per dose, and AG-028262 at 3, 10, 20, or 40 mg/kg body weight per dose. This treatment schedule and route was selected to mimic clinical studies, where axitinib is administered orally twice daily (1), and based on the finding that anti-angiogenesis-induced tumor vascular normalization is typically observed during a 2-7 day period of time following the initial drug treatment (2-4). The impact of these anti-angiogenic agents on the uptake of 4-OH-CPA by 9L tumors was determined as follows. Freshly prepared CPA dissolved in PBS (140 mM NaCl, 10 mM Na$_2$HPO$_4$, 2.7 mM KCl, 1.8 mM KH$_2$PO$_4$) was filtered through a 0.2 µm acrodisc syringe filter (Pall Corp., Ann Arbor, MI) and a single test dose of CPA (either 50 or 140 mg/kg body weight, as indicated) was administered by *i.p.* injection to tumor-bearing mice 24 hr after the last axitinib or AG-028262 treatment. Mice were killed 6 or 15 min after CPA injection, the latter time corresponding to the T$_{max}$ of plasma and liver 4-OH-CPA (5,6). Blood, liver and tumor samples were collected and assayed for 4-OH-CPA and/or CPA, as described below.

In a second treatment schedule, male *scid* mice implanted *s.c.* with 9L/2B11 tumor cells were randomized to different groups on the day of initial drug treatment, when the average tumor volume reached ~ 800 mm^3. This tumor size was chosen to facilitate intratumoral drug delivery. Axitinib was suspended at 5 mg/ml of polyethylene glycol 400 and sonicated at room temperature for 10-20 min to obtain a fine suspension. The suspension was adjusted to pH 2-3 using 0.1 N HCl, sonicated for an additional 20 min, then stored at 4°C in the dark up to 4-5 days. On the day of dosing, a final 3:7 (v/v) ratio of polyethylene glycol 400: H$_2$O was obtained by adding acidified water (pH 2-3) with brief vortexing. Axitinib was administered to the tumor-bearing mice by daily *i.p.* injection at 25 mg/kg body weight and in a volume of 5 µl per g body weight. AG-028262 was prepared as described above and administered at 40 mg/kg body weight per injection (*p.o.*, bid). SU5416 was dissolved in DMSO and injected at 25 mg/kg body weight (*i.p.*, sid). CPA was administered 24 hr after the last anti-angiogenesis treatment, or to untreated

Ma et al, Supplementary Material

controls. Intratumoral delivery of CPA was achieved using a syringe pump (cat. # 70-2212, Harvard Apparatus, Holliston, MA) set to deliver 1 μl per sec. The total CPA dose given to each mouse (50 mg/kg body weight) was dissolved in a volume of ~120 μl PBS and administered intratumorally by injection at three sites per tumor over a period of ~1 min in each of 2 tumors/mouse. Blood, tumor, and liver tissues were collected at times ranging from 5 to 240 min after the last CPA injection, typically for n = 3 mice and n = 6 tumors per time point.

HPLC and MS analysis of CPA and 4-OH-CPA – Tissue samples (tumor, plasma, liver) were processed and analyzed for 4-OH-CPA by HPLC after derivatization (7,8). Tissue recovery of 4-OH-CPA was 60 ± 3% with a sensitivity of 1 μM under these conditions (8). CPA levels in tumor plasma and liver were determined using liquid chromatography-tandem mass spectrometry, essentially as described (9). Briefly, 100 μl of tumor or liver homogenate, or 25 μl of plasma, was mixed with 100 μl of 10 ng/μl or 1 ng/μl ifosfamide solution (internal standard). The sample was adjusted to a total volume of 200 μl, and 800 μl of acetonitrile was added to precipitate the protein. Samples were vortexed and centrifuged and the supernatant was removed and evaporated under a stream of N_2 at 40°C. The pellet was then reconstituted in 100 μl of HPLC mobile phase and stored at –20°C until analysis. CPA was analyzed using a Waters 600 controller coupled to an API 2000 tandem mass spectrometer (Applied Biosystems, Foster City, CA). Chromatography was carried out using a Luna C18(2) column (5 μm, 150 x 3.0 mm) (Phenomenex, Torrance, CA) with an isocratic mobile phase consisting of 35% acetonitrile in 20 mM ammonium acetate buffer (pH 5.0) and a flow rate of 0.4 ml/min. CPA was determined in the positive electrospray ionization mode at 350°C capillary temperature, 5.0 kv ionization voltage, and 20v collision energy. Nitrogen was used as the collision gas at a setting of 12 (arbitrary units). Multiple reaction monitoring data were acquired with the following variables: the CPA transition was m/z 260.9 > 140.1 and ifosfamide was m/z 260.9 > 154.1, with a dwell time of 600 milliseconds for both. Selected ion monitoring was used for CPA (m/z 140.1) and ifosfamide (m/z 154.1); retention times were 4.2 min for CPA and 4.0 min for ifosfamide. CPA was quantified using Analyst software (Applied Biosystems, Foster City, CA). Data are expressed as nmol CPA or 4-OH-CPA per g of tissue (i.e., μM), mean ± SE based on n = 3 individual mice or n = 6 individual tumors per time point.

Pharmacokinetic data analysis - Pharmacokinetics data were analyzed as described (5). Using 6 pharmacokinetic time course data points collected for each of 3 individual mice (3 blood, 3 liver and 6 tumor samples at each time point). Data were randomly assigned into three separate time course data sets for plasma and liver, and six separate time course data sets for the tumors. Each data set was used to calculate AUC, $t_{1/2}$, C_{max} and T_{max} values using WinNonlin software version 1.5 (Scientific Consulting Inc, Apex, NC) with a simple noncompartment model. The initial intratumoral concentration of CPA (at t = 0.5 min) was set to the mean CPA concentration within each of the six tumor samples and was calculated based on the quantity of CPA injected divided by the tumor's weight. Pharmacokinetic parameters were calculated based on with the descriptive statistics module of WinNonlin software. Statistical comparisons using a nonparametric *t*-test were performed using GraphPad Prism software version 4 (GraphPad, Inc., San Diego, CA). Data are expressed as nmol CPA or 4-OH-CPA per g of tissue (i.e., μM), mean ± SE based on n = 3 individual mice or n = 6 individual tumors per time point. CPA 4-hydroxylase activity was assayed in tissues obtained from mice bearing 9L/2B11 tumors treated with vehicle (5 μl per g body weight, *i.p.* sid) or axitinib (25 mg/kg body weight, *i.p.* sid) for 4

days. Twenty four hr after the last drug treatment, microsomes were prepared from fresh tumor tissue and CPA 4-hydroxylase activity was assayed by HPLC following incubation *in vitro* with 0.2 or 2 mM of CPA (6).

Endothelial cell chemosensitivity to 4-OH-CPA - HUVEC cells were grown in EGM-2 culture medium containing 2% FBS at 37°C in a humidified, 5% CO_2 atmosphere. 4-HC, a chemically activated derivative of CPA that spontaneously decomposes to 4-OH-CPA in aqueous solution, was used to assay the chemosensitivity of cultured HUVEC cells to 4-OH-CPA. Cells were treated with one of the following schedules: 1) 4-HC alone at 0 to 100 μM for 4 days; 2) concurrent 4-HC and axitinib (2 μM) for 4 days; 3) two days of axitinib pretreatment followed by 4 days of co-treatment with 4-HC and axitinib. Relative cell number was determined after 4 days by crystal violet staining. Data are expressed as mean ± SE based on n = 3 individual wells per point.

Apoptosis in CPA-induced tumors - Mice bearing 9L/2B11 tumors were treated with one of the following schedules: 1) untreated controls; 2) axitinib (25 mg/kg body weight, *i.p.*, sid, for 4 days) followed by PBS (120 μl/mouse, administered on day 5 at 20 μl per injection at each of 3 intratumoral sites per tumor and 2 tumors/mouse, and repeated on day 6); 3) vehicle (5 μl per g body weight, *i.p.*, sid, for 4 days) followed by CPA (a total of 50 mg CPA/kg body weight, administered on day 5 in a total vol of 120 μl/mouse at 20 μl per injection at each of 3 intratumoral sites per tumor and 2 tumors/mouse, and repeated on day 6); 4) axitinib daily for 4 days followed by CPA on days 5 and 6. Tumors were collected 24 hr after the last intratumoral injection and homogenized in ice-cold KPi buffer (100 mM potassium phosphate, 1 mM EDTA, 1 mM dithiothreitol, 1 mM Na_3VO_4, and 1 tablet of protease inhibitor cocktail/50 ml). Following an initial centrifugation (12,000 rpm in a Beckman Coulter microfuge) for 20 min at 4°C, the supernatant was centrifuged at 35,000 rpm in a Sorval T-1270 rotor for 1 hr at 4°C. Supernatant protein concentrations were determined by Bradford assay. Caspase activity was determined using the Caspase-Glo 3/7 assay kit and the manufacturer's protocol, with the following modifications. Protein samples in a 96-well plate (50 μg in 50 μl) were incubated with 10 μl of potassium phosphate buffer or casputin stock solution (2 mg/ml) at room temparature for 15 min. 60 μl of reconstituted caspase 3/7 substrate was then added to each well. After a brief shaking, the plate was incubated at room temparature for 30 min and luciferase activity was determined using a Victor-3 Multilabel Counter (Perkin Elmer). Caspase 3/7 activity was calculated as the difference of luciferase activity in the presence vs. absence of casputin. Data are expressed as mean ± SE values based on n = 6 individual tumors per treatment group.

References for Supplementary Materials and Methods

1.   Rixe O, Bukowski RM, Michaelson MD, et al. Axitinib treatment in patients with cytokine-refractory metastatic renal-cell cancer: a phase II study. Lancet Oncol 2007; 8: 975-84.
2.   Dickson PV, Hamner JB, Sims TL, et al. Bevacizumab-induced transient remodeling of the vasculature in neuroblastoma xenografts results in improved delivery

and efficacy of systemically administered chemotherapy. Clin Cancer Res 2007; 13: 3942-50.

3.   Wildiers H, Guetens G, De Boeck G, et al. Effect of antivascular endothelial growth factor treatment on the intratumoral uptake of CPT-11. Br J Cancer 2003; 88: 1979-86.

4.   Winkler F, Kozin SV, Tong RT, et al. Kinetics of vascular normalization by VEGFR2 blockade governs brain tumor response to radiation: role of oxygenation, angiopoietin-1, and matrix metalloproteinases. Cancer Cell 2004; 6: 553-63.

5.   Chen CS, Jounaidi Y, Su T, Waxman DJ. Enhancement of intratumoral cyclophosphamide pharmacokinetics and antitumor activity in a P450 2B11-based cancer gene therapy model. Cancer Gene Ther 2007; 14: 935-44.

6.   Ma J, Waxman DJ. Modulation of the antitumor activity of metronomic cyclophosphamide by the angiogenesis inhibitor axitinib. Mol Cancer Ther 2008; 7: 79-89.

7.   Chen CS, Lin JT, Goss KA, He YA, Halpert JR, Waxman DJ. Activation of the anticancer prodrugs cyclophosphamide and ifosfamide: identification of cytochrome P450 2B enzymes and site-specific mutants with improved enzyme kinetics. Mol Pharmacol 2004; 65: 1278-85.

8.   Yu LJ, Drewes P, Gustafsson K, Brain EGC, Hecht JED, Waxman DJ. In vivo modulation of alternative pathways of P450-catalyzed cyclophosphamide metabolism: impact on pharmacokinetics and antitumor activity. J Pharmacol Exp Ther 1999; 288: 928-37.

9.   Pass GJ, Carrie D, Boylan M, et al. Role of hepatic cytochrome p450s in the pharmacokinetics and toxicity of cyclophosphamide: studies with the hepatic cytochrome p450 reductase null mouse. Cancer Res 2005; 65: 4211-7.

10.   Ma J, Waxman DJ. Dominant effect of antiangiogenesis in combination therapy involving cyclophosphamide and axitinib. Clin Cancer Res 2009; 15: 578-88.

Supplementary Figures

Figure S1 - Impact of axitinib treatment on PC-3 tumor uptake of CPA – *Scid* mice bearing *s.c.* PC-3 tumor xenografts with no pretreatment or pretreated with axitinib (25 mg/kg, *i.p.*, sid for 12 hr up to 6 days) were given a test dose of CPA (140 mg/kg, *i.p.*). Levels of CPA in PC-3 tumor were measured at 15 min after CPA administration. Mean ± SE, n = 6 tumors per time point; ** $p < 0.01$ compared to untreated controls. A similar decrease in 4-OH-CPA uptake was previously seen in the same PC-3 tumor samples (10).

Figure S2 - Impact of axitinib on tumor microsomal CPA 4-hydroxylase activity - 9L/2B11 tumor xenografts grown *s.c.* in *scid* mice were pretreated with vehicle or axitinib (25 mg/kg, *i.p.*, sid) for 4 days. Tumor microsomes isolated 24 hr after the last drug treatment were incubated *in vitro* with CPA at a final concentration of either 0.2 or 2.0 mM, as shown. 4-OH-CPA production was determined by HPLC analysis. Mean ± SE, n = 6 tumors per treatment group.

Axitinib: — + — +
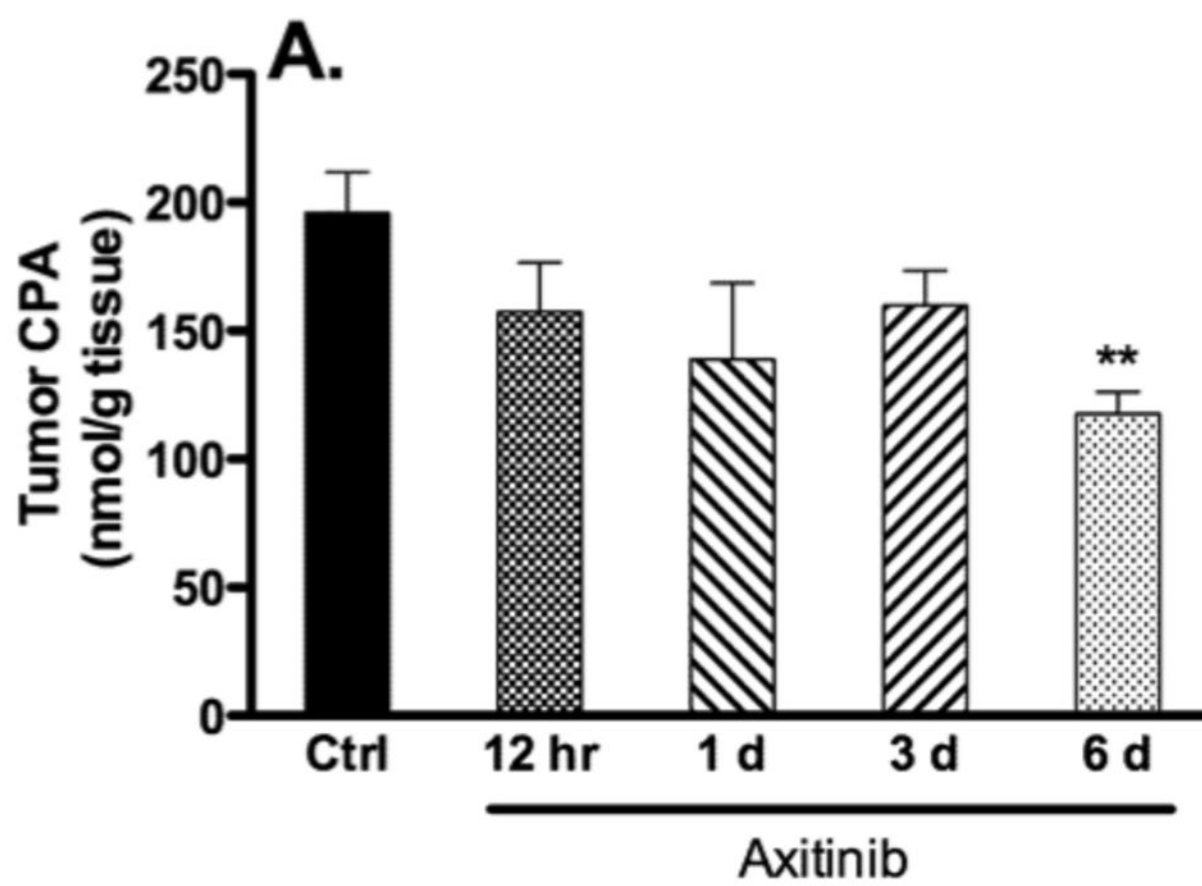
CPA = 0.2 mM   CPA = 2.0 mM